Some aspects of magnetic force computation using BEM-FEM coupling

Joachim Fetzer, Stefan Kurz, Günther Lehner and Wolfgang M. Rucker
Institut für Theorie der Elektrotechnik, Universität Stuttgart, Pfaffenwaldring 47, 70550 Stuttgart, Germany

***Abstract*—For the calculation of magnetic forces with the Maxwell stress tensor the normal and the tangential derivatives of the vector potential $\vec{A}$ have to be known. We choose C^0-continuous elements, therefore $\vec{A}$ and its tangential derivatives are continuous. In contrast, the normal derivative $\partial\vec{A}/\partial n$ calculated with the finite element method is continuous only in a weak sense. When BEM-FEM coupling is used however, the value of $\partial\vec{A}/\partial n$ is uniquely available on the coupling surfaces from the BEM formulation. Two methods of magnetic force computation using $\partial\vec{A}/\partial n$ either from FEM or from BEM data will be presented. Their accuracy will be compared by means of several examples.**

I. BEM-FEM Coupling

Starting from Maxwell-equations describing magnetostatic problems and taking into account the constitutive relation $\vec{B} = \mu_0\vec{H} + \vec{M}$ and the magnetic vector potential $\vec{A}$, the equation

$$-\frac{1}{\mu_0}\vec{\nabla}^2\vec{A} = \vec{g}_s + \frac{1}{\mu_0}\mathrm{rot}\,\vec{M} \tag{1}$$

can be derived. The boundary condition $\vec{A} = 0$ at infinity ensures that the solution of (1) satisfies the Coulomb gauge $\mathrm{div}\,\vec{A} = 0$. The magnetic fields to be calculated are caused by the impressed current density $\vec{g}_s$ and by the magnetization $\vec{M}$.

The domain Ω of the boundary value problem (1) is decomposed into a set of finite element subdomains $\Omega_{\mathrm{FEM}\nu}$ which coincide with the magnetic parts of the problem and a BEM subdomain Ω_{BEM} which represents the surrounding vacuum space and the impressed source currents, Fig. 1. The common boundaries $\Gamma_{\mathrm{FEM}\nu} = \Gamma_{\mathrm{BEMi}\nu}$ correspond to iron-air interfaces.

The application of the finite element method in Ω_{FEM} and the application of the boundary element method in Ω_{BEM} both yield a linear system of equations [1], namely

$$[K]\{\vec{A}^{\mathrm{FEM}}\} - [T]\{\vec{Q}^{\mathrm{FEM}}\} = \{\vec{F}(\vec{M})\}, \tag{2}$$

$$[G]\{\vec{Q}^{\mathrm{BEM}}\} - [H]\{\vec{A}^{\mathrm{BEM}}\} = \{\overrightarrow{RS}(\vec{g}_s)\}. \tag{3}$$

Isoparametric nodal finite elements and boundary elements have been used for the discretization. $\{\vec{A}^{\mathrm{FEM}}\}$ and $\{\vec{A}^{\mathrm{BEM}}\}$ are the nodal values of $\vec{A}$ in $\Omega_{\mathrm{FEM}}\cup\Gamma_{\mathrm{FEM}}$ and on Γ_{BEMi}, respectively. $\{\vec{Q}^{\mathrm{FEM}}\}$ and $\{\vec{Q}^{\mathrm{BEM}}\}$ are the nodal values of

$$\vec{Q} = \frac{1}{\mu_0}\left(\frac{\partial\vec{A}}{\partial n} - \vec{M}\times\vec{n}\right) \tag{4}$$

on $\Gamma_{\mathrm{FEM}} = \Gamma_{\mathrm{BEMi}}$ with $\vec{M} = 0$ in Ω_{BEM}. The boundary values $\{\vec{Q}^{\mathrm{FEM}}\}$, $\{\vec{A}^{\mathrm{BEM}}\}$ and $\{\vec{Q}^{\mathrm{BEM}}\}$ at the nodes on the common boundaries can be eliminated from (2), (3) due to their continuity [2] resulting in

$$\overbrace{\left([K] + [T][G]^{-1}[H]\right)}^{[K']}\{\vec{A}^{\mathrm{FEM}}\} = \underbrace{\{\vec{F}(\vec{M})\} - [T][G]^{-1}\{\overrightarrow{RS}(\vec{g}_s)\}}_{\{\vec{F}'(\vec{g}_s,\vec{M})\}}. \tag{5}$$

The second member vector $\{\vec{F}'\}$ does not depend on the impressed current density $\vec{g}_s$ only, but also on the magnetization $\vec{M}$, specified by the prescribed magnetization

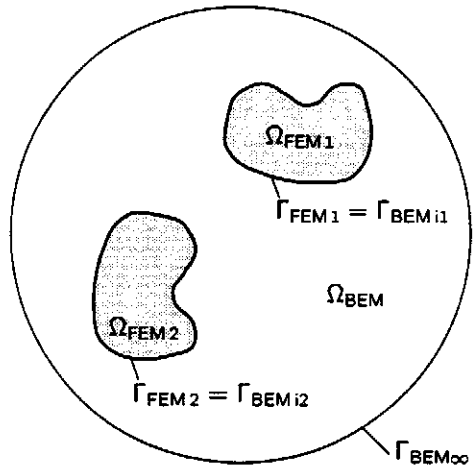

Fig. 1. Structure of the considered domain
$\Omega_{\mathrm{FEM}} = \Omega_{\mathrm{FEM}1} \cup \Omega_{\mathrm{FEM}2}$, $\Omega = \Omega_{\mathrm{FEM}} \cup \Omega_{\mathrm{BEM}}$
$\Gamma_{\mathrm{FEM}} = \Gamma_{\mathrm{FEM}1} \cup \Gamma_{\mathrm{FEM}2}$, $\Gamma_{\mathrm{BEMi}} = \Gamma_{\mathrm{BEMi}1} \cup \Gamma_{\mathrm{BEMi}2}$

Manuscript received September 23, 1996.
J. Fetzer, e-mail joachim.fetzer@ite.uni-stuttgart.de;
S. Kurz, e-mail stefan.kurz@ite.uni-stuttgart.de.

curve. Therefore (5) has to be solved iteratively. In this case, the so-called "combined iteration" [3] which is a variant of the M(B)-iteration has been used.

II. Force Computation

The magnetic force is computed using the well known Maxwell stress tensor (MST) method, i.e. by the integration of a normal and a tangential force density

$$\vec{f}_n = \frac{1}{2}\left(\frac{B_n^2}{\mu_0} - \mu_0 \vec{H}_t^2\right)\vec{n}, \tag{6a}$$

$$\vec{f}_t = B_n \vec{H}_t \tag{6b}$$

over a surface, which entirely encloses the object under consideration,

$$\vec{F} = \oint_S \vec{f}\, \mathrm{d}\Gamma. \tag{7}$$

Considering a Cartesian coordinate system $(\vec{n}, \vec{t}_1, \vec{t}_2)$, which is rotated against the original coordinate system so that $\vec{n}$ is orthogonal to the boundary in the considered point (Fig. 2), the components B_n, H_{t_1} and H_{t_2} are related to the vector potential as follows

$$B_n = \frac{\partial A_{t_2}}{\partial t_1} - \frac{\partial A_{t_1}}{\partial t_2}, \tag{8a}$$

$$H_{t_1} = \frac{1}{\mu}\left(\frac{\partial A_n}{\partial t_2} - \frac{\partial A_{t_2}}{\partial n}\right), \tag{8b}$$

$$H_{t_2} = \frac{1}{\mu}\left(\frac{\partial A_{t_1}}{\partial n} - \frac{\partial A_n}{\partial t_1}\right). \tag{8c}$$

It can be seen from (8a) that B_n is continuous on the boundaries between adjacent finite elements due to the continuity of $\vec{A}$. In contrast, $\vec{H}_t$ is only weakly continuous on such boundaries because it depends on $\partial\vec{A}/\partial n$. The FE formulation satisfies the interface condition for $\partial\vec{A}/\partial n$ resulting from (4) only in a weak sense. Computation of the MST may therefore cause difficulties, because it is not clear, which one of the two different values of $\vec{H}_t$ should be used, especially on iron-air interfaces [4].

In the context of BEM-FEM coupling, it is natural to choose $S = \Gamma_{\mathrm{FEM}\nu} = \Gamma_{\mathrm{BEMi}\nu}$, which means that the integration is actually performed over the iron-air interface

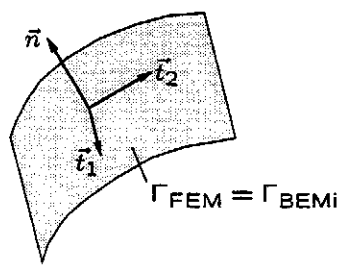

Fig. 2. Local coordinate system $(\vec{n}, \vec{t}_1, \vec{t}_2)$

of the considered part. According to the above, there are two different ways for the computation of the MST. The values of $\partial\vec{A}/\partial n$ can be obtained either from FEM or from BEM data.

A. Computation of the MST by FEM Data (MST FEM)

Introducing the permeability $\mu = 1/\nu$ which may be field dependent, the force density (6) can equivalently be expressed as

$$\vec{f} = \frac{1}{2\mu}\left[(\vec{B}\cdot\vec{n})\vec{B} - (\vec{B}\times\vec{n})\times\vec{B}\right] + \frac{1}{2}(\nu_0 - \nu)\left(B_n^2 + \frac{\nu}{\nu_0}B_t^2\right)\vec{n}. \tag{9}$$

Equation (5) has to be solved before the values of $\vec{B}$ on the boundary $S = \Gamma_{\mathrm{FEM}\nu}$ can be obtained by the usual differentiation of the FE shape functions. The global force can then be calculated with the help of (7) and (9).

B. Computation of the MST by BEM Data (MST BEM)

In the case of $\mu = \mu_0$ like in Ω_{BEM}, the second term in (9) vanishes resulting in

$$\vec{f} = \frac{1}{2\mu_0}\left[(\vec{B}\cdot\vec{n})\vec{B} - (\vec{B}\times\vec{n})\times\vec{B}\right]. \tag{10}$$

The derivatives of $\vec{A}$ with respect to x, y, z are now required to compute $\vec{B} = \mathrm{rot}\,\vec{A}$. From (3), (4) we have $(\vec{M} = 0)$

$$\left\{\frac{1}{\mu_0}\frac{\partial\vec{A}}{\partial n}\right\} = \{\vec{Q}\} = [G]^{-1}\left([H]\{\vec{A}\} + \{\overrightarrow{RS}(\vec{g}_s)\}\right), \tag{11}$$

where the superscripts $^{\mathrm{BEM}}$ have been omitted. Assuming the usual isoparametric nodal boundary elements, $\vec{r}$, $\vec{A}$ and $\vec{Q}$ are interpolated from their nodal values as follows

$$\vec{r} = \sum_{i=1}^{k} N_i(\xi,\eta)\vec{r}_i, \tag{12a}$$

$$\vec{A} = \sum_{i=1}^{k} N_i(\xi,\eta)\vec{A}_i, \tag{12b}$$

$$\vec{Q} = \sum_{i=1}^{k} N_i(\xi,\eta)\vec{Q}_i, \tag{12c}$$

where ξ, η are the local coordinates, N_i the shape functions and k the number of nodes of the boundary element. The derivatives of (12a) are

$$\vec{r}_\xi = \sum_{i=1}^{k} \frac{\partial N_i(\xi,\eta)}{\partial\xi}\vec{r}_i, \tag{13a}$$

$$\vec{r}_\eta = \sum_{i=1}^{k} \frac{\partial N_i(\xi,\eta)}{\partial\eta}\vec{r}_i. \tag{13b}$$

TABLE I
COMPUTATIONAL DATA FOR THE HOLLOW SPHERE

	Coarse Mesh Linear Elements	Fine Mesh Linear Elements	Coarse Mesh Quadratic Elements	Analytical [5]
Total number of nodes	555	2499	3369	-
Number of FEM elements	1978	9726	1920	-
Number of boundary nodes	242	882	882	-
Number of BEM elements	400	1600	400	-
Total number of equations	1255	6039	8649	-
Force F_z by MST BEM	341.83 N	364.55 N	372.90 N	372.88 N
Force F_z by MST FEM	339.84 N	363.87 N	372.81 N	372.88 N

The unit normal vector is

$$\vec{n} = \frac{\vec{r}_\xi \times \vec{r}_\eta}{|\vec{r}_\xi \times \vec{r}_\eta|} = \frac{\partial \vec{r}}{\partial n}. \tag{14}$$

Application of

$$\begin{pmatrix} \partial x \\ \partial y \\ \partial z \end{pmatrix} = J^{-1} \begin{pmatrix} \partial \xi \\ \partial \eta \\ \partial n \end{pmatrix}, \tag{15}$$

$$J = (\vec{r}_\xi \quad \vec{r}_\eta \quad \vec{n})^T \tag{16}$$

allows the calculation of the desired derivatives from (12). The global force can then again be calculated with the help of (7) and (10).

III. NUMERICAL EXAMPLES

In this section, two numerical examples are presented to compare the computed forces of both methods (MST FEM, MST BEM) with each other and with analytical or measured values. Both examples are modelled with the coupled BEM-FEM scheme of Fig. 1, where the BEM region is air.

A. Magnetic Attraction of a Ferromagnetic Sphere

This problem is discussed in [5] and has an analytical solution. A hollow ferromagnetic sphere is placed under a circular current loop, which exerts an attractive force on it. The parameters are given in Fig. 3. For symmetry reasons only a quarter of the sphere needs to be discretized. Computations have been performed with linear elements (3-noded triangles, 6-noded tetrahedrons) as well as quadratic elements (6-noded triangles, 10-noded tetrahedrons) and with two different meshes. Fig. 4 shows the coarse and Fig. 5 the fine BE mesh. Some computational data and the results for the attractive force are summarized in Table I. Both methods yield nearly identical forces. Especially the computation based on quadratic

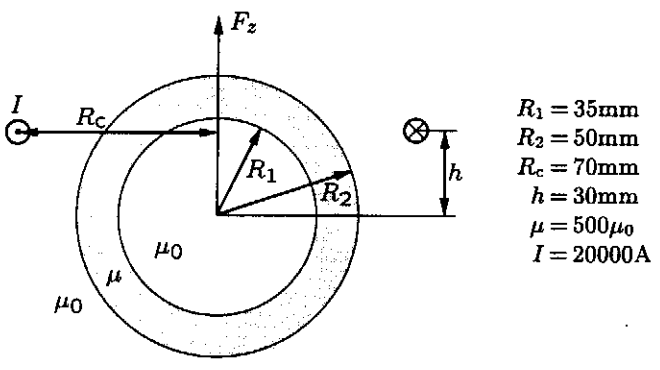

Fig. 3. Magnetic attraction of a hollow sphere

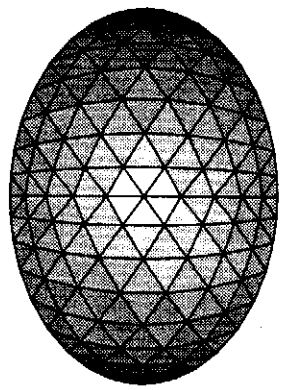

Fig. 4. Coarse discretization of $^1/_4$ of the hollow sphere

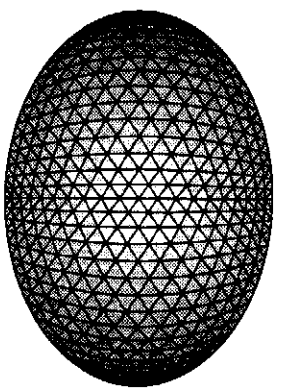

Fig. 5. Fine discretization of $^1/_4$ of the hollow sphere

elements gives excellent results. The reason for this might be that quadratic isoparametric elements are better suited for the modelling of a smooth surface.

B. TEAM Workshop Problem 20

As a second example we consider TEAM Workshop problem 20, which consists of a steel center pole surrounded by an exciting coil. The magnetic circuit is completed by a steel yoke. A complete definition of the geometry can be found in [6]. Taking advantage of the symmetry, only a quarter of the problem region had to be discretized using 8-noded quadratic quadrilaterals and 20-noded quadratic hexahedrons, Fig. 6. Some computational data are given in Table II. The measured and computed values of the force F_z acting on the center pole can be seen from Table III and Fig. 7. Again, there is good agreement between both methods and the measured data.

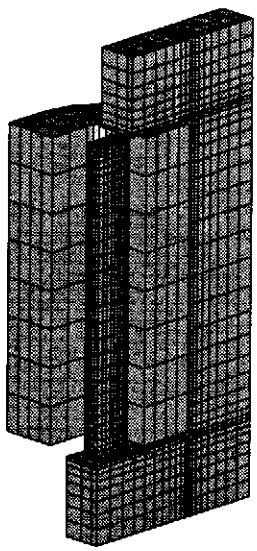

Fig. 6. Discretization of $^1/_4$ of TEAM problem 20

TABLE II
COMPUTATIONAL DATA FOR TEAM PROBLEM 20

Total number of nodes	15068
Number of FEM elements	2784
Number of boundary nodes	4266
Number of BEM elements	1346
Total number of equations	38231

TABLE III
FORCE F_z ACTING ON THE CENTER POLE

Excitation	Measured [7]	MST BEM	MST FEM
1000 AT	7.8 N	8.7 N	8.4 N
3000 AT	54.3 N	56.8 N	54.5 N
4500 AT	75.5 N	76.0 N	73.6 N
5000 AT	81.0 N	81.4 N	78.7 N

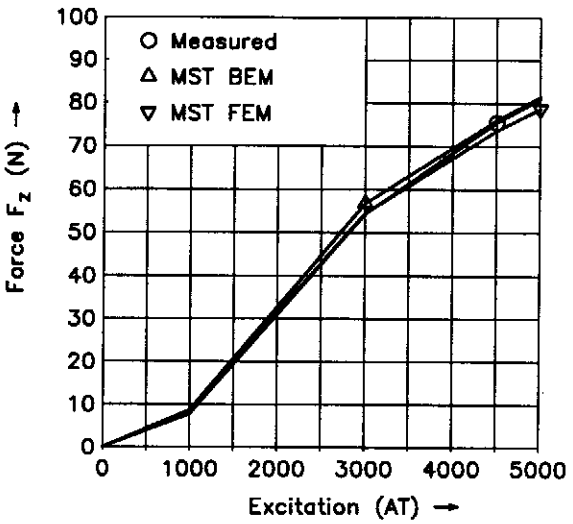

Fig. 7. Force F_z acting on the center pole of TEAM problem 20

IV. CONCLUSIONS

Two methods have been presented for the evaluation of the Maxwell stress tensor in the context of BEM-FEM coupling. It has been demonstrated that a good accuracy can be achieved even when the surface of integration coincides with the iron-air interface provided that the discretization is appropriate. In connection with BEM-FEM coupling, the MST method is easy to implement in an existing code, because no additional surfaces have to be introduced for the integration.

REFERENCES

[1] J. Fetzer, *The solution of static and quasistationary electromagnetic field problems using the coupling of finite elements and boundary elements (in German)*, PhD thesis, Universität Stuttgart, VDI Verlag Düsseldorf, 1995.

[2] J. Fetzer, S. Kurz, and G. Lehner, "Comparison between different formulations for the solution of 3D nonlinear magnetostatic problems using BEM-FEM coupling", *IEEE Transactions on Magnetics*, vol. 32, no. 3, pp. 663–666, May 1996.

[3] S. Kurz, J. Fetzer, and G. Lehner, "A novel iterative algorithm for the nonlinear BEM-FEM coupling method", *IEEE Transactions on Magnetics*, in press.

[4] A.N. Wignall, A.J. Gilbert, and S.J. Yang, "Calculation of forces on magnetized ferrous cores using the Maxwell stress method", *IEEE Transactions on Magnetics*, vol. 24, no. 1, pp. 459–462, Jan. 1988.

[5] Z. Ren, "Comparison of different force calculation methods in 3D finite element modelling", *IEEE Transactions on Magnetics*, vol. 30, no. 5, pp. 3471–3474, Sept. 1994.

[6] T. Nakata, N. Takahashi, H. Morishige, J.L. Coulomb, and C. Sabonnadiere, "Analysis of 3-D static force problem", in *Proc. of TEAM Workshop on Computation of Applied Electromagnetics in Materials*, Sapporo, Japan, 1993, pp. 73–79.

[7] T. Nakata, N. Takahashi, M. Nakano, H. Morishige, and K. Matsubara, "Improvement of measurement of 3-D static force problem", in *Proc. of the 4th International TEAM Workshop*, Miami, Nov. 1993, pp. 133–135.